



SEISMIC SOURCE MECHANISM CHARACTERISTICS OBSERVED DURING THE BAMBANANI MINE SHAFT PILLAR EXTRACTION

S van der Wath

Rock Engineering Manager, Harmony Bambanani Gold Mine

J Mohlatsane

General Manager, Harmony Bambanani Gold Mine

J Gerber

Head of Seismology and Numerical Modelling (Africa), Institute of Mine Seismology

SYNOPSIS

Bambanani mine management undertook a seismic source moment tensor analysis project of large seismic events within the shaft pillar, to improve the understanding into the sources of these large seismic events. This data has proven to be invaluable in understanding the change in source mechanism of seismic events at the mine. The damage observed underground in the Bambanani Shaft pillar stoping excavations, after the occurrence of some large seismic events, accentuated a change in the rockburst source mechanism. Prior to June 2021 the majority of large seismic events were either pillar, abutment or structure driven. The major change in seismic source mechanism was observed from June 2021, when severe damage and face ejection was observed in stoping panels. The stope was exposed to the dynamic deformation process as part of the seismic source volume. Rockburst damage was also characterized by partial and/or total closure of panels and gullies. Stopping excavations approaching holing into shaft infrastructure on reef elevation, was highlighted using numerical modelling, as the main contributor to the initial change in the seismic source mechanism. Another change in the seismic response also transpired as panel faces were mined in line, which resulted in shear failure on the face abutments.



INTRODUCTION

General overview of Bambanani mine shaft pillar extraction

Mine Name	Bamabanani East Mine (Previously President Steyn Nr. 4 Mine)
Location	Welkom, Free State
Shaft Infrastructure	Serviced by East shaft (Services, men and material), West shaft (Ore hoisting and backfill), Decline shaft and Chairlift
Reef	Basal reef
Depth below surface	1883m – 2211m
Mining Method	Scattered mining layouts and mini long wall sequencing
Dip span, strike span and area of the pillar	707m * 667m = 471 569m ²
Footwall Development (Reef Access)	Old shaft infrastructure and newly developed ends within the 60° overstoped shadow
Stoping width	Undercut – 1.8m Open cut – 2.5m (Average)
Dip	35° (Average)
Hanging wall rock	Undercut – Basal quartzite (Fractured hanging wall beam below the Khaki shale) Open cut – Waxy Brown / Leader Quartzite (Geological complex hanging wall with ball and pillow features)
Footwall rock	Upper Formation 1 – Zone 1 Footwall quartzite
Regional Support	Regional stability pillars with cemented backfill
In stope Support	Cemented backfill, rapid yielding hydraulic props, tendons (Not in undercut panels), steel netting and welded mesh (In gullies).
Seismic Network	Institute of Mine Seismology (IMS) network, consisting of 10*4.5Hz three component geophones underground as well as 4*1Hz three component geophone surface sites. The network has a sensitivity of Mmin -1.0 and a location accuracy of 20m.

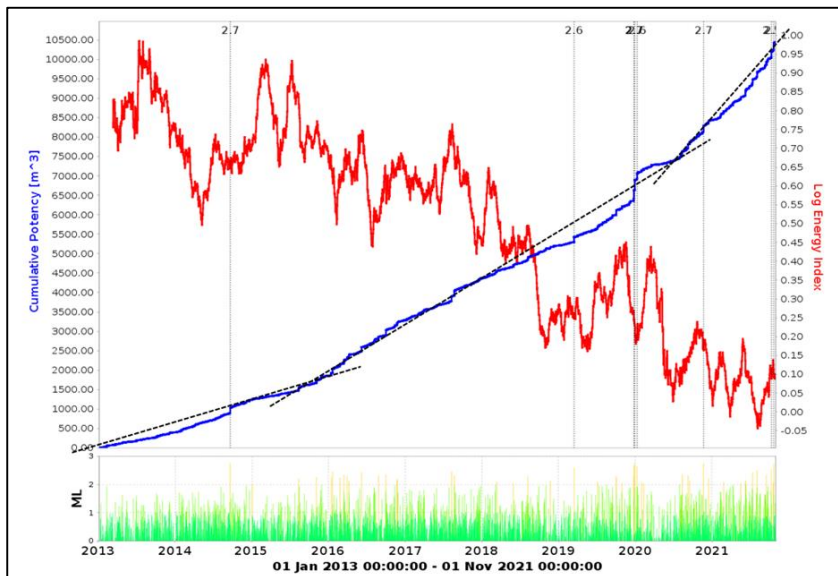
Table 1: Bamabanani East Mine shaft pillar characteristics.

Main challenge at Bamabanani mine

Dynamic rockmass response to mining is the major challenge faced by the Bamabanani team during the extraction of the shaft pillar. Numerical modelling, seismic hazard risk assessments and underground observations indicated faulting, pillars and abutments to present the main seismic risk to the shaft pillar extraction. This rapidly changed when observations different to the norm were made underground after the occurrence of some large seismic events, which highlighted a change in the seismic source mechanism.



SEISMIC ANALYSIS OF THE SHAFT PILLAR EXTRACTION



Graph 1: Time history of Cumulative Potency and Energy Index for the shaft pillar extraction. Seismic events $>ml2.5$ are also indicated on the graph.

Evident from the graph, is a decrease in Energy index and an increase in the Cumulative Potency. From 2019 onwards the larger seismic events occurred when the pillar started losing its ability to maintain stress, as was also found by Jager and Ryder (1999).

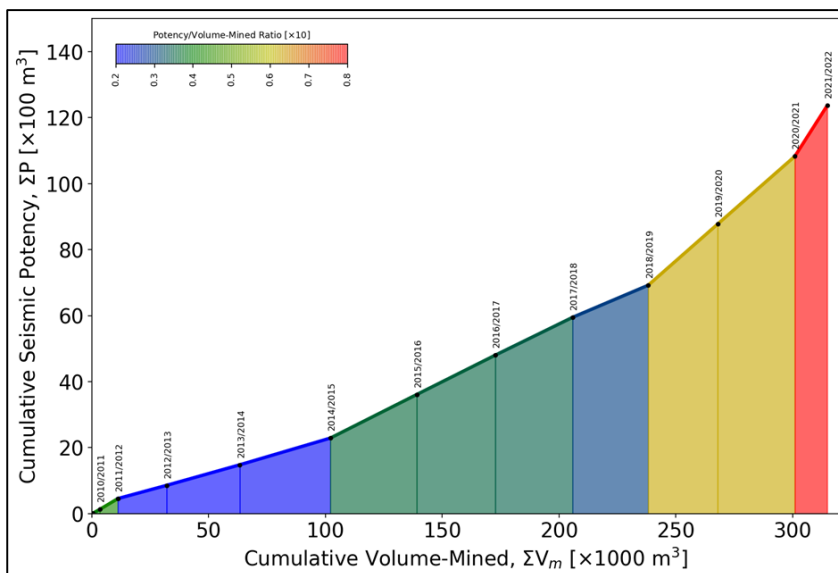


Figure 1: Cumulative seismic potency versus cumulative volume mined for the shaft pillar extraction for the period 2010 – 2022.

Discernible from the figure above, is the increase in Potency versus Volume mined to the latter part of the pillar extraction.

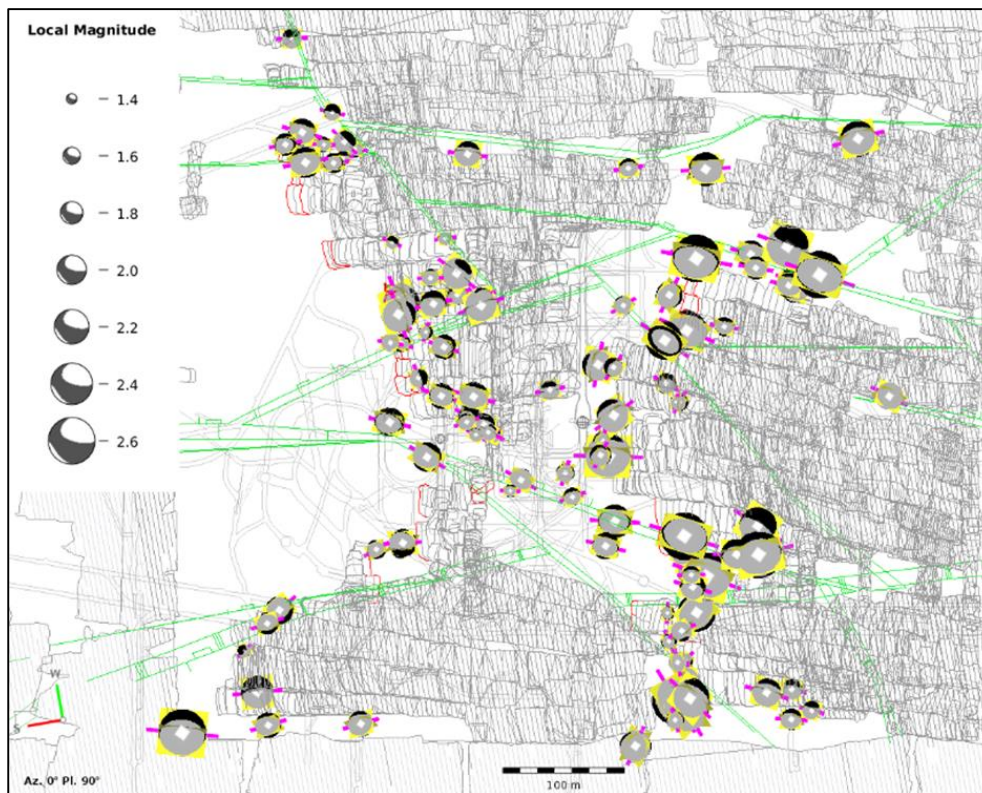


Figure 2: Seismic source mechanism moment tensor analysis plot of all seismic events $>M1.5$ in the shaft pillar for the period 2019 – 2021.

CONTEXTUALIZING SEISMIC SOURCE MECHANISM MOMENT TENSOR ANALYSIS

Classification of seismic source and damage mechanisms

Basic seismic failure mechanisms consist of crush and shear type failure, with three fundamental rockburst types distinguished by Cai & Kaiser (2018), fault slip, pillar burst and strain burst. A more detailed breakdown of the general seismic source mechanisms can be seen in the table below:

seismic source mechanism					
event type	strain burst	buckling	face-crush, pillar burst	shear rupture	fault-slip
local magnitude	-0.2-0	0-1.5	1.0-2.5	2.0-3.5	2.5-5.5 ^a
instability process	spalling, buckling	Euler-type instability	slabbing, crushing, dilation	stick-slip release of energy from strained rock around slip surface	
postulated source mechanism	implosive	implosive	implosive plus shear	double-couple fault-slip	
required condition for event to occur	superficial spalling with violent ejection of fragments	outward expulsion of large slabs pre-existing parallel to surface of opening	sudden collapse of pillar or violent expulsion of large volume of rock from tabular tunnel face	violent propagation of shear fracture through intact rock mass	violent renewed movement on existing fault of dyke contact
required condition for event to occur	failure very close to free surface	free surface \gg lamina thickness	stress $>$ strength in destroyed volume	shear stress $>$ shear strength of rock	shear stress $>$ resistance to sliding
Brune slip model applicable	no	no	no	yes	

Table 2: Modified classification of seismic event sources identified in South African mines. (Linzer, Hildyard & Wesseloo, 2021)



Jager & Ryder (1999) classify rockburst damage mechanisms as, 'Violent shakedown bursts', 'Shakedown bursts' and 'Near-field bursts'. The latter work of Cai & Kaiser (2018) differentiate between four dynamic damage mechanisms, 'sudden stress induced fracturing or strain bursting due to tangential straining of the excavation', 'rock ejection due to a high rock mass bulking rate during strain bursting', 'rock ejection by energy transfer from a remote seismic source' and 'shakedown or falls of ground due to acceleration forces elevated by the impact of ground motions from a remote seismic event'.

Seismic source mechanism moment tensor analysis methodology

A moment tensor analysis is used to represent the source of a seismic event. (Tierney, 2019) Seismic source mechanism can be estimated using ground motion wave forms, which are inverted to a Moment tensor. This inversion of the seismic source mechanism can be done in one of two ways, Polarity and amplitude or Full-waveform source mechanism inversion. The full-waveform inversion is employed for Bambanani mine. The formula of Aki and Richards (2002) can be referenced below:

$$u_n = M_{pq} * G_{np,q}$$

u_n = Displacement

M_{pq} = Moment Tensor

$G_{np,q}$ = Green function

Using this mathematical method, the moment tensor can be inverted, using the displacement which is known and the Green function which is approximated.

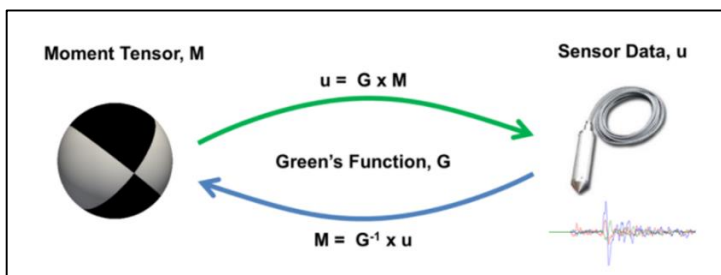


Figure 3: Illustration of a moment tensor inversion when the inverse Green's function is used to find the source moment tensor based on the sensor data. (Tierney, 2019)

A moment tensor can be broken down into a combination of three distinct components: The Isotropic (ISO) component representing the uniform volume change, the Double couple (DC) component referring to shear dislocation and the Compensated Linear Vector Dipole (CLVD) component indicating axial deformation.



	Moment tensor	Beachball	Moment tensor	Beachball	
Black – Compressional quadrants	$\frac{1}{\sqrt{3}} \begin{pmatrix} 1 & 0 & 0 \\ 0 & 1 & 0 \\ 0 & 0 & 1 \end{pmatrix}$		$-\frac{1}{\sqrt{3}} \begin{pmatrix} 1 & 0 & 0 \\ 0 & 1 & 0 \\ 0 & 0 & 1 \end{pmatrix}$		ISO – Explosion / Implosion
	$\frac{1}{\sqrt{2}} \begin{pmatrix} 0 & 1 & 0 \\ 1 & 0 & 0 \\ 0 & 0 & 0 \end{pmatrix}$		$\frac{1}{\sqrt{2}} \begin{pmatrix} 1 & 0 & 0 \\ 0 & -1 & 0 \\ 0 & 0 & 0 \end{pmatrix}$		
White – Dilatational quadrants	$\frac{1}{\sqrt{2}} \begin{pmatrix} 0 & 0 & -1 \\ 0 & 0 & 0 \\ -1 & 0 & 0 \end{pmatrix}$		$\frac{1}{\sqrt{2}} \begin{pmatrix} 0 & 0 & 0 \\ 0 & 0 & -1 \\ 0 & -1 & 0 \end{pmatrix}$		
	$\frac{1}{\sqrt{2}} \begin{pmatrix} -1 & 0 & 0 \\ 0 & 0 & 0 \\ 0 & 0 & 1 \end{pmatrix}$		$\frac{1}{\sqrt{2}} \begin{pmatrix} 0 & 0 & 0 \\ 0 & -1 & 0 \\ 0 & 0 & 1 \end{pmatrix}$		Compensated Linear Vector Dipole
	$\frac{1}{\sqrt{6}} \begin{pmatrix} 1 & 0 & 0 \\ 0 & -2 & 0 \\ 0 & 0 & 1 \end{pmatrix}$		$\frac{1}{\sqrt{6}} \begin{pmatrix} -2 & 0 & 0 \\ 0 & 1 & 0 \\ 0 & 0 & 1 \end{pmatrix}$		

Figure 4: ‘Beach ball’ illustrations of different moment tensors, linked to different moment tensor components. (Anthony, 2011).

The moment tensor analysis referenced below, refers to examples of past seismic events at Bamabanani mine and consist of, Total = ISO + CLVD + DC:

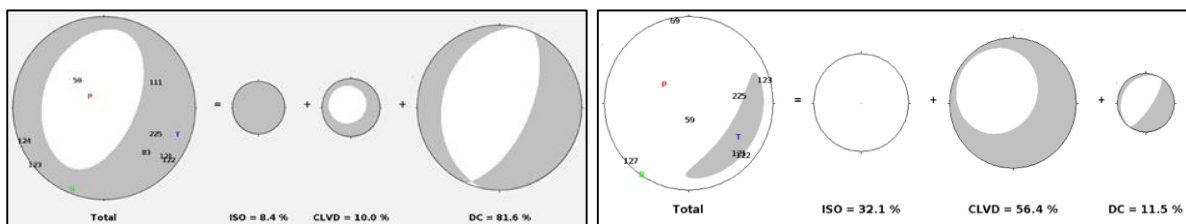


Figure 5 & 6: Moment tensor beach ball composition examples, left having a large DC component indicating a fault-slip mechanism and right having large ISO and CLVD components indicating a crush type mechanism and change in volume.

“The Hudson chart is a useful tool to visualize the moment tensor decomposition, seeing the relative proportions of the isotropic, DC and CLVD elemental sources.” (Tierney, 2019)

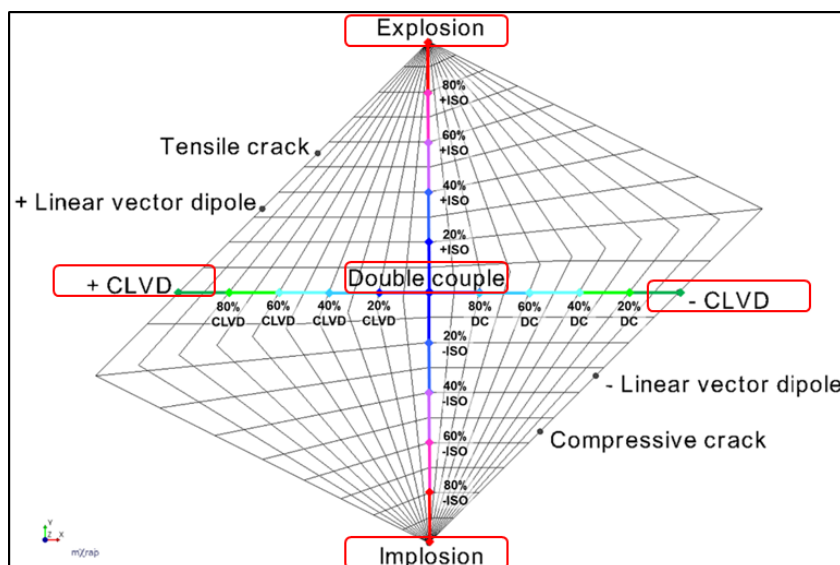


Figure 7: Hudson diagram (Equal area source type plot) as described by Tierney (2019) can be used to plot moment tensor analysis.

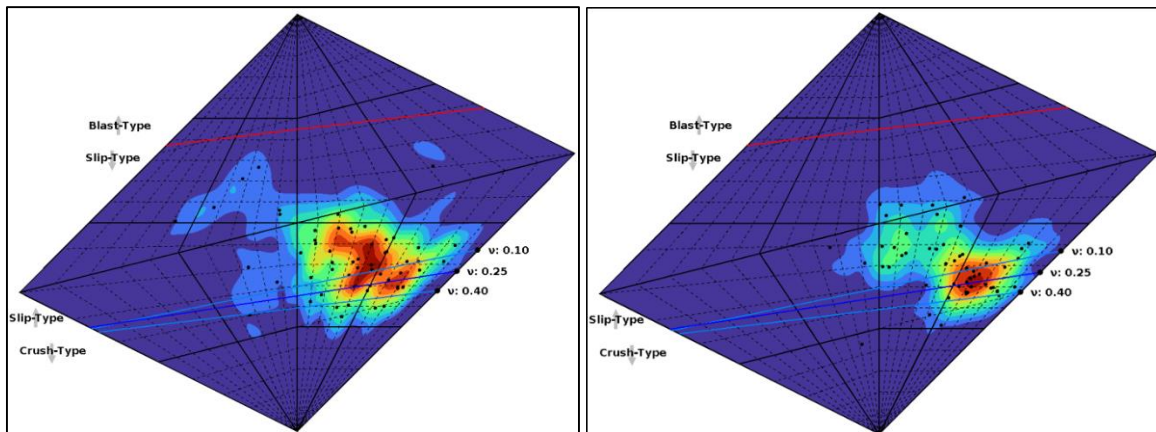


Figure 8 & 9: Hudson diagrams for seismic events >ml1.5 for the period 2019 – 2020 and 2021.

Using the Hudson diagram to plot the moment tensor analysis, the 'hotspot' contour has shifted slightly downwards, which indicates that a larger percentage of events are now 'crush-type', rather than 'slip-type'.

SEISMIC EVENT CASE STUDIES

Pillar burst case study – 5th August 2020 ml1.6

On 5th August 2020 a ml1.6 seismic event occurred at the 71-80 raise line. The seismic event plot and associated moment tensor analysis can be seen below:

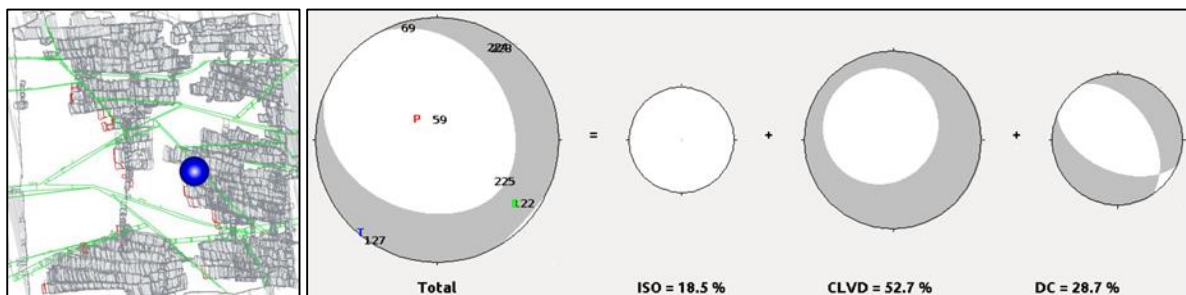


Figure 10 & 11: Ml1.6 seismic event plot at the 71-80 raise line and its moment tensor analysis.

The ISO and CLVD components suggest crush type deformation within the source region.



Photo 1: Underground observations panel 71-80 S9 panel face.

Rockburst damage was observed in panel S9 as rock ejected from the panel face. Panel S9 was lagging its top and bottom panels, thus isolating the S9 panel.

Fault slip case study – 22nd November 2020 ml2.7

On 22nd November 2020 a ml2.7 seismic event occurred at the 71-80 raise line. The seismic event plot and associated moment tensor analysis can be seen below:

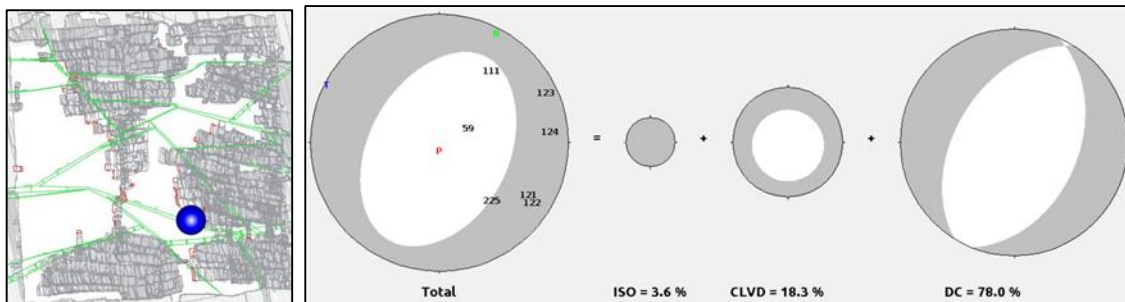


Figure 12 & 13: ML2.7 seismic event plot at the 71-80 raise line and its moment tensor analysis. The estimated source mechanism has a dominant double couple component.



Photo 2 & 3: Underground observations panel 71-80 S3 gully hanging wall (Left) and panel face (Right).



Photo 4 & 5: Underground observations panel 71-80 S4 panel back area (Left) and panel face (Right).

Rock burst damage was observed in the gully and face of panels S3 and S4. Shakedown from the hanging wall was suspended in the netting, supported by props and backfill. Falls of ground also occurred in the face between the last line of support and the face.

Shear rupture case study – 30th March 2021 ml1.9

On 30th March 2021 a ml1.9 seismic event occurred at the 69-86 raise line. The seismic event plot and associated moment tensor analysis can be seen below:

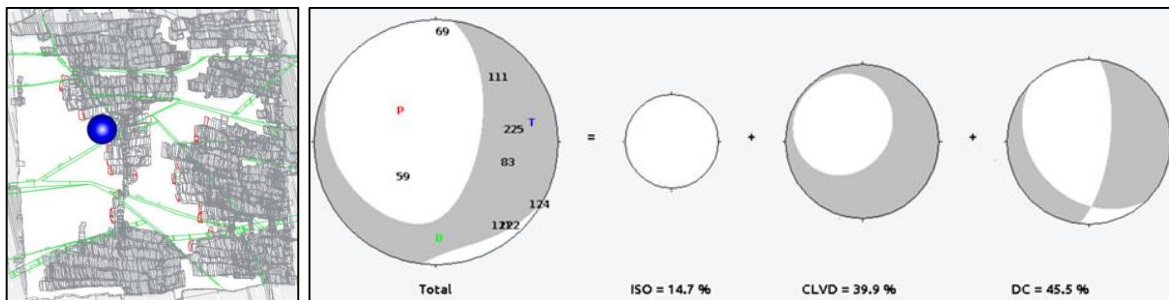


Figure 14 & 15: Ml1.9 seismic event plot at the 69-86 raise line and its moment tensor analysis.

The DC component is dominant suggesting a shear type deformation within the source region.



Photo 6: Underground observations panel 69-86 S9 gully.



Rockburst damage was observed in panel S9 gully and siding. Scattered falls of ground was observed suspended in steel netting and welded mesh in the gully and siding. The lead/lag distance between panels S9 and S8 was excessive which resulted in the abutment failure.

List of damaging seismic events (June 2021 onwards)

DATE	RAISE LINE & PANEL	EVENT MAGNITUDE	SOURCE MECHANISM	DAMAGE	CASE STUDY
9 Jun 2021	71-80 S9, S7	2.1	Pillar burst (# Infrastructure)	Violent shake down and face ejection	Pillar burst case study 1
9 Jun 2021	71-80 S5	2.1	Fault slip	Shake down	
12 Jul 2021	Main Shaft	1.9	Pillar burst (# Infrastructure)	Ejection into shaft barrel	
18 Sep 2021	69-86 S9, S8	2.3	Shear Rupture (Faces in line)	Violent shake down and face ejection	Shear rupture case study 1
25 Sep 2021	69-80 Crosscut	1.9	Pillar burst	Violent shake down, sidewall ejection & footwall heave	
11 Oct 2021	71-80 S6, S5	2.4	Pillar burst (# Infrastructure)	Violent shake down and face ejection	Pillar burst case study 2
22 Oct 2021	69-80 S5	2.7	Fault slip	Shake down	
3 Nov 2021	71/73-80	2.6	Complex	Violent shake down	
26 Nov 2021	69-80 S5, S4	1.9	Shear Rupture (Faces in line)	Violent shake down	
13 Jan 2022	71-80 S4, S3	1.7	Shear Rupture (Faces in line)	Shake down and face ejection	Shear rupture case study 2
14 Jan 2022	69-86 S3	2.2	Shear Rupture (Abutment)	Violent shakedown	

Table 3: List of damaging seismic events and its associated source classification from Jun 2021 – Jan 2022.

Pillar burst case study one – 9th June 2021 ml2.1

On 9th June 2021 a ml2.1 seismic event occurred at the 71-80 raise line. The seismic event plot and associated moment tensor analysis can be seen below:

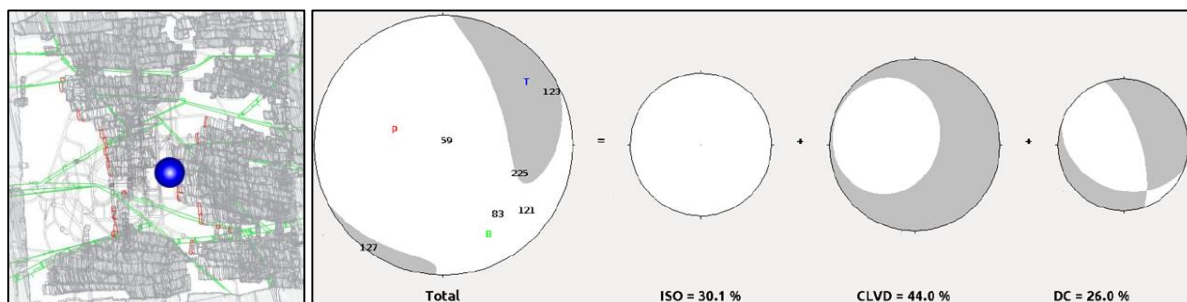


Figure 16 & 17: Ml2.1 seismic event plot at the 71-80 raise line and its moment tensor analysis. The ISO and CLVD components suggest crush type deformation within the source region.



Photo 7 & 8: Underground observations panel 71-80 S7 gully face (Left) and panel face (Right).

Severe rockburst damage was observed in panel S7 with falls of ground observed in the gully and face, with the full face length of the panel ejecting. Rock flour can be seen on the fracture planes in the photo of the gully face hanging wall, indicating the close proximity to the rupture process within the source region. Gully tendons dislodged with the hanging wall rock in the gully. Hydraulic props and steel cable netting kept the panel face open, but large volumes of rock were suspended in the netting from the hanging wall and from the face.

Pillar burst case study two – 11th October 2021 ml2.4

On 11th October 2021 a ml2.4 seismic event occurred at the 71-80 raise line. The seismic event plot and associated moment tensor analysis can be seen below:

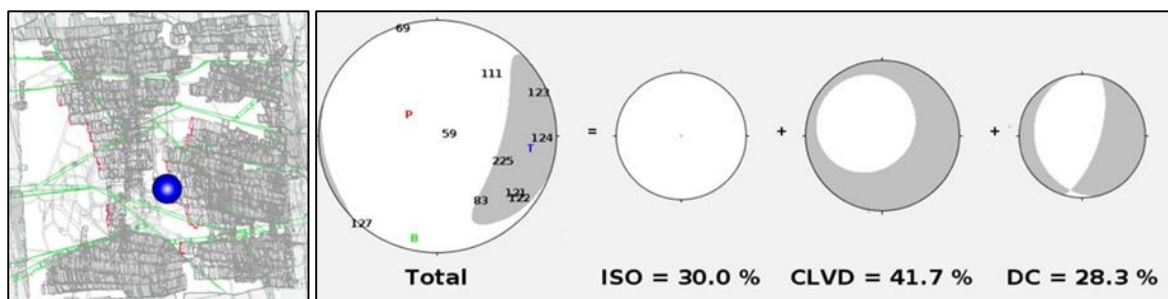


Figure 18 & 19: ML2.4 seismic event plot in the shaft pillar and its moment tensor analysis.

The large ISO and CLVD components suggest a crush type failure mechanism.



Photo 9 & 10: Underground observations panel 71-80 S6 gully (Left and Right).



Photo 11 & 12: Underground observations panel 71-80 S6 panel face (Left and Right).

Severe rockburst damage was observed in the gully and in the face of the panel, to such an extent that access into the gully (10m back from the gully face) and panel face (toe and mid panel) was not possible. Rock flour was noted on fracture planes in the gully hanging wall, indicating the close proximity to the rupture process within the source region. Gully packs were dislodged into the gully, with hanging wall rocks ejected next to tendons and a hanging wall tendon observed to be bent during dynamic loading. Face ejection with blasted ore from the face and a subsequent fall of ground from the hanging wall, closed the panel face. The total destruction of a headboard observed in the face substantiates the close proximity to the source region. Hydraulic props were shifted back during the event by the face ejection, shifting the blasted ore. The hanging wall beam broke up between props and resulted in significant net sagging up to the blasted ore and ejected rock from the face.

Numerical modelling was done to analyse the stress state around the stoping excavation

Numerical modelling was done using the Institute of Mine Seismology (IMS) Vantage modelling software (Boundary Element Method). Numerical modelling was done after the m12.4 seismic event.



Parameters used in the model:

Datum (m):	483
Young's Modulus (GPa):	70
Poisson's Ratio:	0.2
Stress Tensor Sxx (MPa/m):	0.014
Stress Tensor Syy (MPa/m):	0.014
Stress Tensor Sxx (MPa/m):	0.028
Backfill Model:	Hyperbolic

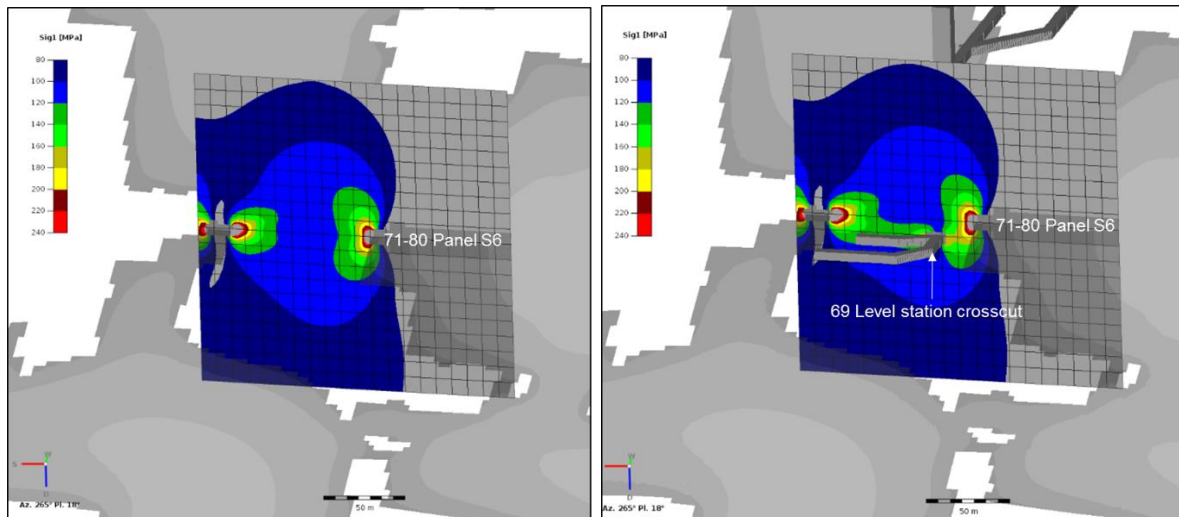


Figure 20 & 21: Vertical sheet of the Sigma 1 stress on the 71-80 S6 panel with and without 69 level shaft infrastructure included.

Initial planning of the shaft pillar extraction was to sacrifice the Main and Sub shafts and its infrastructure below 60 level, which included large excavations like hoist rooms, shaft barrels, shaft stations, dams and crosscuts. Monthly numerical modelling was conducted of the shaft pillar mining, but this only included stoping excavations and did not indicate any anomalous conditions. When adding the shaft infrastructure excavations into the model the Sigma 1 stress lobe interaction between the stoping and the shaft infrastructure becomes apparent, as seen from the figures above. The holing into the shaft infrastructure is thus not only a holing risk, but also a seismic risk as the isolated block between the excavations is overstressed, especially in the final remnant with elevated levels of stress.

Shear rupture case study one – 18th September 2021 ml2.3

On 18th September 2021 a ml2.3 seismic event occurred at the 69-86 raise line. The seismic event plot and associated moment tensor analysis can be seen below:

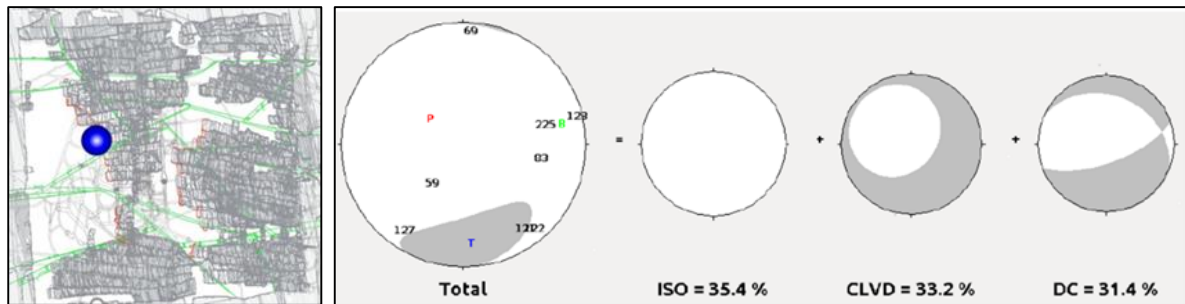


Figure 22 & 23: MI2.3 seismic event plot in the shaft pillar and its moment tensor analysis.

The nodal planes of the DC component align with the panel faces. ISO and CLVD components also suggest volumetric type deformation within the source region.



Photo 13 & 14: Underground observations panel 69-86 S9 face toe (Left) and face top (Right).

Severe rockburst damage was observed in the gully and in the face of the panel, to such an extent that the toe of the panel could not be accessed. The full face length of the panel ejected increasing in intensity as observed on the stretch of face nets, towards the bottom of the panel. Footwall heave was observed on the footwall of the panel. Hanging wall rock ejected next to tendons in the gully. The hydraulic props in the bottom which could be observed from the back area, were shifted out of position by the rock from the face ejection. This resulted in the hanging wall in the toe of the panel, to fall. The severity of the observed face ejection in the bottom of the panel confirms the close proximity to the source region.

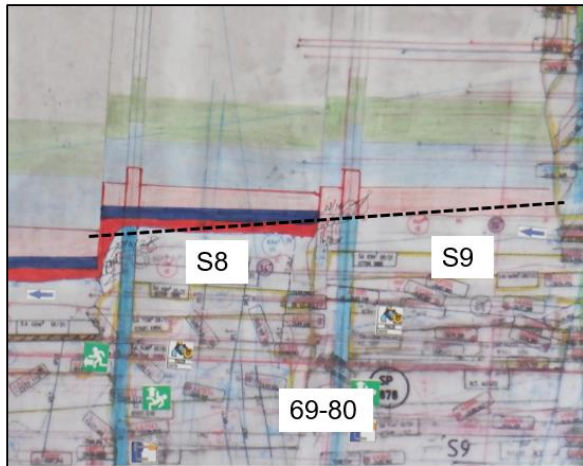


Photo 15: Stopping panel face configuration in line, forcing shear rupture on the face abutment.

Shear rupture case study two – 13th January 2021 ml1.7

On 13th January 2022 a ml1.7 seismic event occurred at the 71-80 raise line. The seismic event plot and associated moment tensor analysis can be seen below:

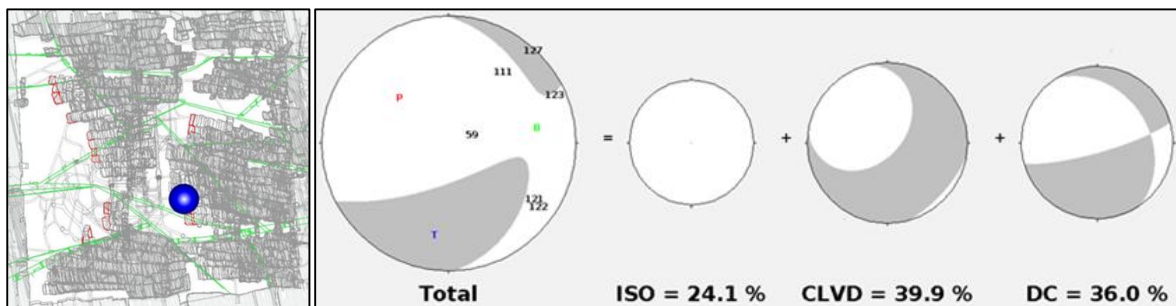


Figure 24 & 25: Ml1.7 seismic event plot in the shaft pillar and its moment tensor analysis.

The nodal planes of the DC component align with the panel faces and the ISO and CLVD components suggest some volumetric type deformation within the source region.



Photo 16 & 17: Underground observations panel 71-80 S3 face (Left) and S4 face (Right).

Rockburst damage was observed on both the panel faces. Large slabs loosened on S3 panel face and the face in panel S4 ejected. Hydraulic props and face netting secured all the ejected rock. The significant damage on panel S4 face is expected as this is close to the source region.



Photo 18: Stopping panel face configuration in line, forcing shear rupture on the face abutment.

CONCLUSION

The importance of seismic source mechanism moment tensors as tool to analyse and understand larger and normally damaging seismic events, must be stressed as a critical aspect to distinguish between the drivers of these seismic events on mines. Five source mechanisms were distinguished during the shaft pillar extraction, with the analysis also making it possible to track the migration of source mechanisms making use of the Hudson diagram. Understanding the source mechanism is pivotal for appropriate controls to be put in place to mitigate the seismic risk. Stopes approaching holing into shaft infrastructure were seen as a holing risk, but it was also emphasized to also be a seismic risk. It is thus important that shaft infrastructure excavations are included in the numerical modelling, to determine the stress state around these excavations, to relate it back to rock strength and determine a failure criterion.

Observations made from moment tensor analysis during the shaft pillar extraction, again confirmed that large magnitude events are associated with geological structures and that there is a correlation, between the size of the ISO component of the moment tensors and the underground damage. This is expected as the ISO component do represent a volume change. This highlights the importance of proper underground investigations of areas affected by these seismic events.

To ensure stable and reliable results when performing moment tensor inversions, the seismic system should be designed to provide: 1) reasonable location accuracy of larger seismic events; and 2) coverage of the corresponding seismic sources ("focal spheres") in all directions as far as reasonably possible. It is the opinion of the authors that the location accuracy of larger seismic events (e.g. events with magnitude $m_l > 0.0$) should be 50 m or better and at least ten fully-operational, three-component/tri-axial sensors should be available for performing moment tensor inversions. Also, it is important to ensure that all sensors are correctly installed, as the orientation of sensors can significantly affect the stability and reliability of the moment tensor results (e.g. unintended rotation of a seismic sensor in the borehole during installation).

Future work should investigate a 'source driven' seismic monitoring system criteria, required for moment tensor analysis. It is also of importance to ensure that the rock engineering personnel on the shaft has the enhanced skill and ability to manage seismic data driven projects and programs.



REFERENCES

- Aki, K. and Richards, P. 2002. *Quantitative Seismology*. Second Ed. University Science Books.
- Anthony, R. 2011. *An Introduction to Non-Double-Couple Sources*. Department of Earth and Environmental Science, New Mexico Institute of Mining and Technology.
- Cai, M. and Kaiser, P. K. 2018. *Rockburst Support Reference Book. Volume 1: Rockburst Phenomenon and Support Characteristics*. MIRARCO – Mining Innovation, Laurentian University.
- Hedley, D.G.F. 1992. *Rockburst handbook for Ontario hard rock mines*. CANMET Special Report SP92-1E. 305.
- Hudson, J.A., Pearce, R.G. and Rogers, R.M. 1989. *Source Type Plot for Inversion of the Moment Tensor*. JOURNAL OF GEOPHYSICAL RESEARCH, VOL. 94
- Jager, A.J. and Ryder, J.A., 1999. *Rock Engineering Practice for tabular hard rock mines*. The Safety in Mines Research Advisory Committee (SIMRAC).
- Linzer, L.M., Hildyard, M.W. and Wesseloo, J. 2021. *Complexities of underground mining seismic sources*. The Royal Society.
- Malovichko, D. and Van Aswegen, G. 2013. *Testing of the Source Processes of Mine Related Seismic Events*. 8th Int. Symp. On Rockbursts and Seismicity in Mines.
- Malovichko, D. 2020. *Description of Seismic Sources in Underground Mines: Theory*. Bulletin of the Seismological Society of America.
- Mendecki, A. J. 2016. *Mine Seismology Reference Book: Seismic Hazard*. Institute of Mine Seismology.
- Ryder, J.A. and Jager, A.J. 2002. *Rock Mechanics for Tabular Hard Rock mines*. The Safety in Mines Research Advisory Committee (SIMRAC).
- Tierney, S. 2019. *Moment Tensor – A Practical Guide*. <https://mxrap.com/moment-tensors-a-practical-guide/>